Joint Estimation of TOA and DOA in IR-UWB System Using Sparse Representation Framework

Fangqiu Wang and Xiaofei Zhang

This paper addresses the problem of joint time of arrival (TOA) and direction of arrival (DOA) estimation in impulse radio ultra-wideband systems with a two-antenna receiver and links the joint estimation of TOA and DOA to the sparse representation framework. Exploiting this link, an orthogonal matching pursuit algorithm is used for TOA estimation in the two antennas, and then the DOA parameters are estimated via the difference in the TOAs between the two antennas. The proposed algorithm can work well with a single measurement vector and can pair TOA and DOA parameters. Furthermore, it has better parameter-estimation performance than traditional propagator methods, such as, estimation of signal parameters via rotational invariance techniques algorithms matrix pencil algorithms, and other new joint-estimation schemes, with one single snapshot. The simulation results verify the usefulness of the proposed algorithm.

Keywords: Impulse radio ultra wideband, time of arrival, direction of arrival, orthogonal matching pursuit, propagator method, estimation of signal parameters via rotational invariance techniques.

Manuscript received June 13, 2013; revised Sept. 22, 2013; accepted Nov. 21, 2013.

This work was supported by China NSF Grants (61371169, 61071164), Jiangsu Planned Projects for Postdoctoral Research Funds (1201039C), China Postdoctoral Science Foundation (2012M521099, 2013M541661), Open Project of Key Laboratory of Underwater Acoustic Communication and Marine Information Technology (Xiamen University), Hubei Key Laboratory of Intelligent Wire1ess Communications (IWC2012002), Open Project of Key Laboratory of Modern Acoustic of Ministry of Education (Nanjing University), the Aeronautical Science Foundation of China (20120152001), Research Innovation Program for College Graduates of Jiangsu Province (CXZZ13_0165), Funding for Outstanding Doctoral Dissertation in NUAA (BCXJ13-09), Qing Lan Project, priority academic program development of Jiangsu High Education Institutions and the Fundamental Research Funds for the Central Universities (NZ2012010, NS2013024, kfjj130114).

Fangqiu Wang (phone: +86 15150555082, wangfangqiu.2008@163.com) and Xiaofei Zhang (zhangxiaofei@nuaa.edu.cn) are with the College of Electronic and Information Engineering, Nanjing University of Aeronautics and Astronautics, Nanjing, China.

I. Introduction

Impulse radio ultra-wideband (IR–UWB) has recently attracted considerable interest for indoor geolocation and sensor networks due to its intrinsic properties, such as immunity to multipath fading, extremely short duration pulse, being carrier free, having a low-duty cycle, wide bandwidth, and low-power spectral density [1]–[5]. On account of the high time resolution nature, UWB positioning based on time-of-arrival (TOA) estimation methods becomes a superior alternative. Furthermore, if direction of arrival (DOA) can also be estimated in the positioning system it would reduce the number of reference nodes needed to estimate the position of UWB sources.

Recently the joint estimation of TOA and DOA is a hot topic in IR-UWB communication systems, and many techniques have been proposed to obtain accurate TOA and DOA estimates. In [6] and [7], TOA estimation was accomplished by using a matched filter but had strong practical limitations due to the requirement of extremely high sampling rates and complexity. To reduce the complexity at sub-Nyquist sampling rates, the non-coherent algorithms based on energy detection were proposed in [8] and [9]. However, the precision of the TOA estimates decreased. Besides, the above algorithms consider the TOA estimation as a timing acquisition problem; TOA estimation was also linked to frequency domain and to super-resolution techniques such as the multiple signal classification (MUSIC) algorithm [10], [11], minimum-norm algorithm [12] and propagator method (PM) [13]. These algorithms are applied after the estimated channel-impulse response is transformed to frequency domain and offers high-resolution TOA estimation. However, the estimators obtain the TOA estimates by spectral peak searching, which has high

http://dx.doi.org/10.4218/etrij.14.0113.0555

complexity and large computation. In other works, such as [14], a union-of-subspaces approach was proposed to recover the time delays and time-varying gain coefficients of each multipath component from low-rate samples of the received signal.

In addition to TOA, DOA is also one of the significant parameters in UWB communication systems, and the problem of DOA estimation has attracted considerable attention in earlier literatures. In [15], a frequency-domain MUSIC algorithm was presented for the estimation and tracking of UWB signals. In [16], the iterative quadratic maximum likelihood algorithm was applied to yield DOA estimates in UWB communication systems. In [17], a beamspace-based DOA estimation method for direct-sequence UWB signals was proposed using the frequency-domain frequency-invariant beamformers algorithm. DOA estimators, however, cannot explicitly exploit the advantage of the large bandwidth of UWB signals. Actually, TOA and DOA are closely related and can be jointly estimated [18]–[21]. In [18], the matrix pencil algorithm was extended to joint TOA and DOA estimation for UWB positioning. The scheme proposed in [19] performs timing acquisition following a two-step approach: a coarse TOA estimator based on a minimum distance criterion, and a fine TOA estimator based on calculation of power delay profile and the selection of a suitable threshold. Finally, the DOA is obtained from the independent TOA measurements at each array antenna by means of a linear estimator. In [20], the joint TOA and angle-of-arrival (AoA) estimator utilizes an array of antennas, each feeding a demodulator consisting of a squarer and a low-pass filter. Signal samples, taken at Nyquist rate at the filter outputs, are processed to produce TOA and AoA estimates. In [21], a joint space-time technique for UWB signals based on the extended MUSIC algorithm was presented. All those joint TOA and DOA estimation methods extract the DOA estimation from the TOA, and because of the high time nature of the UWB signals, DOA estimates can be obtained with reasonable accuracy.

Compressed sensing (CS), which is a novel theory introduced in [22], [23], unifies signal sensing and compression into a single task and can recover the sparse signal with high probability, from a set of random linear projections using nonlinear reconstruction algorithms. In addition to the signal reconstruction and restoration [22], [23], the CS framework has also been applied to UWB communication systems for signal detection, channel estimation, and TOA estimation [24]–[32]. In this paper, we propose a joint TOA and DOA estimation algorithm for IR-UWB signals, based on the sparse representation framework, with a two-antenna receiver. After transforming the received signals to the frequency domain, the estimation problems are linked to the sparse representation framework. Exploiting this link, an orthogonal matching pursuit (OMP) algorithm is used for TOA estimation in the two antennas, and then DOA parameters are estimated via the difference of the TOAs between the two antennas. The proposed algorithm can work well with one single snapshot and can pair TOA and DOA parameters. Furthermore, it has better parameter-estimation performance than the traditional PMs, such as, estimation of signal parameters via rotational invariance techniques (ESPRIT) algorithm, matrix pencil algorithm, and other, new, joint schemes in [19] and [20], with a single measurement vector (SMV). The simulation results verify the usefulness of the proposed algorithm.

The remainder of this paper is structured as follows. Section II develops the data model, and section III presents the proposed algorithm. The Cramér-Rao bound (CRB) of the joint estimation performance is derived in section IV. In section V, simulation results are presented to verify the improvements for the proposed algorithm, while our conclusions are shown in section VI.

Notation: Bold lowercase letters represent vectors and bold uppercase letters represent matrices. The symbols $(\bullet)^*, (\bullet)^T, (\bullet)^H$, $(\bullet)^{-1}$ and $(\bullet)^+$ denote the complex conjugation, transpose, conjugate-transpose, inverse, and pseudo-inverse, respectively. The symbol $\| \|_F$ stands for Frobenius norm. A diagonal matrix whose diagonal is the vector $\mathbf{v}$ is represented by diag($\mathbf{v}$). We denote an estimated expression by $\hat{(\bullet)}$.

II. Data Model

We assume that each information symbol is typically implemented by the repetition of N_c short pulses with modulation of direct-sequence binary phase-shift keying (DS-BPSK). The transmitted signal can be represented as

$$s(t) = \sum_{i=-\infty}^{+\infty} \sum_{n=0}^{N_c-1} b_i c_n p(t - iT_s - nT_c), \quad (1)$$

where $b_i \in \{-1, +1\}$ and $c_n \in \{-1, +1\}$ are the information symbols and the user-specific code sequence, respectively. The pulse waveform is referred to as $p(t)$, which is the second derivative of a Gaussian pulse with T_s being the symbol duration and T_c being the chip duration. The transmitted UWB signal passes through a multipath channel, which is modeled, as in [33], by

$$h(t) = \sum_{k=1}^{K} \beta_k \delta(t - \tau_k), \quad (2)$$

where β_k and τ_k are the fading coefficient and the propagation delay of the kth path, respectively. Without loss of generality, we assume $\tau_1 < \tau_2 < \cdots < \tau_K$. The Dirac Delta

function is represented by $\delta(t)$, and K is the number of multipath components. Thus, the received signal can be expressed as the summation of multiple delayed and attenuated replicas of the transmitted signal plus the additive Gaussian white noise $w(t)$, that is

$$y(t)=\sum_{k=1}^{K}\beta_k s(t-\tau_k)+w(\mathrm{t})\,. \tag{3}$$

Performing a Fourier transformation on the received signal in (3), we can obtain

$$Y(\omega)=\sum_{k=1}^{K}\beta_k S(\omega)e^{-j\omega\tau_k}+W(\omega)\,, \tag{4}$$

where $Y(\omega)$, $S(\omega)$, and $W(\omega)$ denote the Fourier transformation of $y(t)$, $s(t)$, and $w(t)$, respectively. Then, sampling (4) at $\omega_m = n\Delta\omega$, for $m = 0, 1, \ldots, M-1$ and $\Delta\omega = 2\pi/M\,(M > K)$, and rearranging the frequency samples $Y(\omega)$ into vector $\mathbf{y} = [Y(\omega_0)\ \ldots\ Y(\omega_{M-1})]^T \in \mathbb{C}^{M\times 1}$, yields the frequency domain signal model

$$\mathbf{y} = \mathbf{S}\mathbf{E}_\tau\boldsymbol{\beta} + \mathbf{w}\,, \tag{5}$$

where $\mathbf{S} \in \mathbb{C}^{M\times M}$ is a diagonal matrix whose components are the frequency samples $S(\omega_m)$, and $\mathbf{E}_\tau = [\mathbf{e}(1)\ \ldots\ \mathbf{e}(K)] \in \mathbb{C}^{M\times K}$ is a delay matrix with the column vectors being $\mathbf{e}(k) = [1\ e^{-j\Delta\omega\tau_k}\ \ldots\ e^{-j(M-1)\Delta\omega\tau_k}]^T$ for $k = 1, \ldots, K$. The channel-fading coefficients are arranged in the vector $\boldsymbol{\beta} = [\beta_1 \ldots \beta_K]^T \in \mathbb{C}^{K\times 1}$, and the noise samples are arranged in vector $\mathbf{w} = [W(\omega_0)\ \ldots\ W(\omega_{M-1})]^T \in \mathbb{C}^{M\times 1}$.

III. Joint Estimation of TOA and DOA

1. The Strategy for Joint Estimation of TOA and DOA

The UWB signal $s(t)$ propagates through the K-path fading channel and arrives at an array consisting of two antennas, which is shown in Fig. 1.

Assume that τ_k and ς_k are the TOAs of the kth path in antenna 1 and antenna 2 for $k = 1, \ldots, K$. According to the above data model, the received signals in the frequency domain of each antenna can be expressed as

$$\mathbf{y}_1 = \mathbf{S}\mathbf{E}_\tau\boldsymbol{\beta} + \mathbf{w}_1\,, \tag{6}$$

$$\mathbf{y}_2 = \mathbf{S}\mathbf{E}_\varsigma\boldsymbol{\beta} + \mathbf{w}_2\,, \tag{7}$$

where $\mathbf{S} = \mathrm{diag}([S(\omega_0)\ \ldots\ S(\omega_{M-1})])$ is a diagonal matrix whose components are the frequency samples of transmitted UWB signal $s(t)$. The delay matrices $\mathbf{E}_\tau$ and $\mathbf{E}_\varsigma$ can be denoted by

$$\mathbf{E}_\tau = \begin{bmatrix} 1 & 1 & \cdots & 1 \\ e^{-j\Delta\omega\tau_1} & e^{-j\Delta\omega\tau_2} & \cdots & e^{-j\Delta\omega\tau_K} \\ \vdots & \vdots & \ddots & \vdots \\ e^{-j(M-1)\Delta\omega\tau_1} & e^{-j(M-1)\Delta\omega\tau_2} & \cdots & e^{-j(M-1)\Delta\omega\tau_K} \end{bmatrix} \tag{8}$$

and

$$\mathbf{E}_\varsigma = \begin{bmatrix} 1 & 1 & \cdots & 1 \\ e^{-j\Delta\omega\varsigma_1} & e^{-j\Delta\omega\varsigma_2} & \cdots & e^{-j\Delta\omega\varsigma_K} \\ \vdots & \vdots & \ddots & \vdots \\ e^{-j(M-1)\Delta\omega\varsigma_1} & e^{-j(M-1)\Delta\omega\varsigma_2} & \cdots & e^{-j(M-1)\Delta\omega\varsigma_K} \end{bmatrix}, \tag{9}$$

where $\boldsymbol{\beta} = [\beta_1 \ldots \beta_K]^T \in \mathbb{C}^{K\times 1}$ represents the channel-fading coefficients. Noise samples of antenna 1 and antenna 2 are arranged in $\mathbf{w}_1 = [W_1(\omega_0)\ \ldots\ W_1(\omega_{M-1})]^T \in \mathbb{C}^{M\times 1}$ and $\mathbf{w}_2 = [W_2(\omega_0)\ \ldots\ W_2(\omega_{M-1})]^T \in \mathbb{C}^{M\times 1}$, respectively.

Let $\widehat{\Delta\tau_k} = \widehat{\tau_k} - \widehat{\varsigma_k}$, which is the difference of the TOAs associated to the kth path. From Fig. 1, we get

$$\mathrm{c}\times\widehat{\Delta\tau_k} = d\sin\theta_k\,, \tag{10}$$

with θ_k being the DOA of the kth path, d the distance between the two antennas, and c the speed of light. According to (10), we can obtain the closed-form solution of θ_k, that is

$$\widehat{\theta_k} = \arcsin\left(\frac{\mathrm{c}\times\widehat{\Delta\tau_k}}{d}\right),\ k = 1, \cdots, K. \tag{11}$$

From (11), we know that to obtain the estimation of DOAs, we must estimate the multipath delays in the two antennas first. So, in the following subsection, we will present the method to estimate the TOAs.

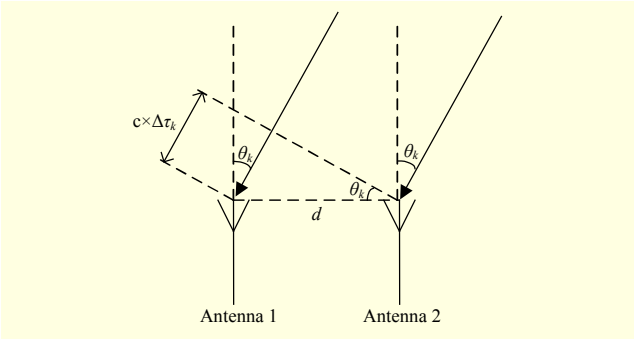

Fig. 1. A two-antenna receiver for joint TOA and DOA.

2. TOA Estimation Based on Sparse Representation

In this subsection, we formulate the TOA estimation problem as a sparse representation problem. To solve (6) and (7) with a sparse representation, we generalize the delay matrices $\mathbf{E}_\tau$ and $\mathbf{E}_\varsigma$ to an overcomplete dictionary $\mathbf{E}$ in terms of all possible TOAs $\{\widehat{\tau_1}, \widehat{\tau_2}, \ldots, \widehat{\tau_N}\}$ with $\widehat{\tau_1} < \widehat{\tau_2} < \cdots < \widehat{\tau_N}$, such that

$$\mathbf{E} = \left[\mathbf{e}(\widehat{\tau_1})\quad \mathbf{e}(\widehat{\tau_2})\quad \ldots\quad \mathbf{e}(\widehat{\tau_N})\right], \tag{12}$$

http://dx.doi.org/10.4218/etrij.14.0113.0555

with N being the grid number, and $N >> K$, $N >> M$. Note that $\mathbf{E}$ is known and does not depend on the actual multipath arrival times τ_k and ς_k in this framework. Thus, the channel-fading coefficients vector $\boldsymbol{\beta}$ can be extended to an $N\times1$ vector $\mathbf{h}$, where the nth element h_n is nonzero and equal to β_k if the arrival time of the kth multipath component is $\widehat{\tau}_n$ and zero otherwise. It means that we can estimate the TOA as long as we find the position of nonzero values in $\mathbf{h}$. Using the overcomplete dictionary $\mathbf{E}$, (6) and (7) become

$$\mathbf{y}_1 = \mathbf{SEh}_1 + \mathbf{w}_1, \tag{13}$$

$$\mathbf{y}_2 = \mathbf{SEh}_2 + \mathbf{w}_2. \tag{14}$$

Note, that we consider an SMV, that is, a single snapshot in the paper. Let $\boldsymbol{\Psi} = \mathbf{SE}$ and we have

$$\mathbf{y}_1 = \boldsymbol{\Psi}\mathbf{h}_1 + \mathbf{w}_1, \tag{15}$$

$$\mathbf{y}_2 = \boldsymbol{\Psi}\mathbf{h}_2 + \mathbf{w}_2. \tag{16}$$

For this case, $\mathbf{h}_1$ and $\mathbf{h}_2$ are sparse vectors which can be used to improve the TOAs estimation. To use the sparse property as a constraint, we utilize the l_0 norm to arrive at the following optimization:

$$\widehat{\mathbf{h}_1} = \arg\min_{\mathbf{h}_1} \|\mathbf{h}_1\|_{l_0} \quad \text{s.t.} \quad \|\mathbf{y}_1 - \boldsymbol{\Psi}\mathbf{h}_1\|_2^2 \le \varepsilon, \tag{17}$$

$$\widehat{\mathbf{h}_2} = \arg\min_{\mathbf{h}_2} \|\mathbf{h}_2\|_{l_0} \quad \text{s.t.} \quad \|\mathbf{y}_2 - \boldsymbol{\Psi}\mathbf{h}_2\|_2^2 \le \varepsilon, \tag{18}$$

where $\|\mathbf{h}\|_{l_0}$ counts the number of nonzero entries in $|\mathbf{h}|$, and ε is the maximum acceptable error. These problems can be solved by linear programming techniques, such as in the sparse approximation algorithm OMP. The major advantages of this algorithm are its speed and its ease of implementation [34]. The OMP algorithm tries to recover the signal by finding in the measurement signal the strongest component, removing it from the signal, and searching the dictionary again for the strongest atom that is presented in the residual signal. The detailed recovery processing via the OMP algorithm is shown in Fig. 2.

Input:

An $M\times M$ diagonal matrix $\mathbf{S}$.

An $M\times N$ overcomplete dictionary $\mathbf{E}$.

An M-dimensional data vector $\mathbf{y}$.

Output:

An estimate $\hat{\mathbf{h}}$.

A set containing k elements from $\{1,\ldots,N\}$.

An M-dimensional approximation $\mathbf{a}_m$ of the data $\mathbf{y}$.

An M-dimensional residual $\mathbf{r}_k = \mathbf{y} - \mathbf{a}_k$.

Procedure:

1) Initialize the residual $\mathbf{r}_0 = \mathbf{y}$, the index set $\Lambda_0 = \varnothing$, and the iteration counter $t = 1$.

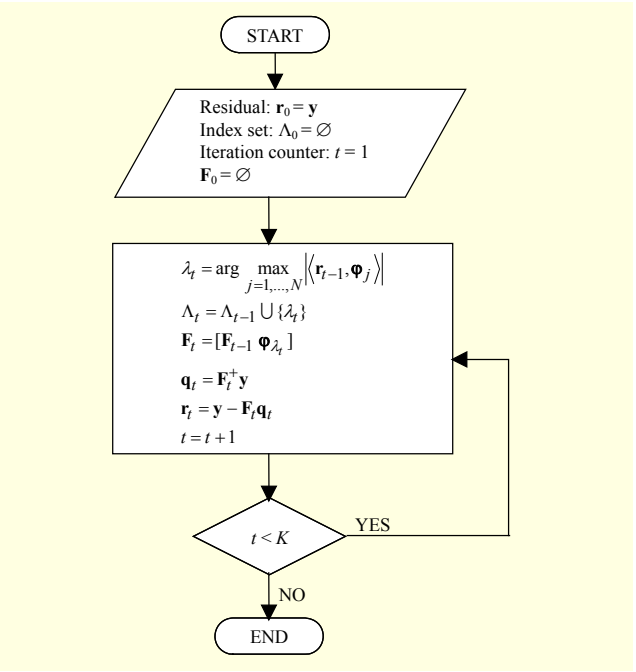

Fig. 2. Flowchart of OMP algorithm.

2) Find the index λ_t that solves the easy optimization problem $\lambda_t = \arg\max_{j=1,\cdots,N} \left|\langle \mathbf{r}_{t-1}, \boldsymbol{\varphi}_j \rangle\right|$, where $\boldsymbol{\varphi}_j$ is the jth column vector of $\boldsymbol{\Psi}$. If the maximum occurs for multiple indices, break the tie deterministically.

3) Augment the index set and the matrix of chosen atoms $\Lambda_t = \Lambda_{t-1} \cup \{\lambda_t\}$ and $\mathbf{F}_t = \left[\mathbf{F}_{t-1} \quad \boldsymbol{\varphi}_{\lambda_t}\right]$. We use the convention that $\mathbf{F}_0$ is an empty matrix.

4) Solve a least-squares problem to obtain a new signal estimate $\mathbf{q}_t = \mathbf{F}_t^+ \mathbf{y}$.

5) Calculate the new approximation of the data $\mathbf{a}_t = \mathbf{F}_t \mathbf{q}_t$ and the new residual $\mathbf{r}_t = \mathbf{y} - \mathbf{a}_t$.

6) Increment t, and return to step 2) if $t < K$.

7) The estimate $\hat{\mathbf{h}}$ for the ideal signal, has nonzero indices at the components listed in Λ_k. The value of the estimate $\hat{\mathbf{h}}$ in component λ_j equals the jth component of $\mathbf{q}_t$.

The two K-sparse vectors $\mathbf{h}_1$ and $\mathbf{h}_2$ can be recovered by the above OMP algorithm, and TOA estimates in the two antennas can be equivalent to finding the sufficiently sparse $\mathbf{h}_1$ and $\mathbf{h}_2$ provided that the error terms are well suppressed. The TOA estimations $\{\widehat{\tau}_k\}_{k=1}^K$ and $\{\widehat{\varsigma}_k\}_{k=1}^K$ are determined from the sparse structure by plotting $\mathbf{h}_1$ and $\mathbf{h}_2$ on the grid of time samples.

3. Pair Matching of TOA in Two Antennas

Since the estimated multipath delays $\{\widehat{\tau}_k\}_{k=1}^K$ and $\{\widehat{\varsigma}_k\}_{k=1}^K$ are obtained independently, we should associate these estimates

so that we can get the DOA estimates via (11). From (6), (7), (13) and (14) we know that the channel-fading coefficients vector $\boldsymbol{\beta}$ is extended to two K-sparse vectors $\mathbf{h}_1$ and $\mathbf{h}_2$, which can be expressed as

$$\mathbf{h}_1 = \left[\mathbf{0}\ h_{1,1}\ \mathbf{0}\ h_{1,2}\ \mathbf{0}\ \ldots\ \mathbf{0}\ h_{1,K}\ \mathbf{0}\right], \tag{19}$$

$$\mathbf{h}_2 = \left[\mathbf{0}\ h_{2,1}\ \mathbf{0}\ h_{2,2}\ \mathbf{0}\ \ldots\ \mathbf{0}\ h_{2,K}\ \mathbf{0}\right]. \tag{20}$$

Actually, the nonzero elements in $\mathbf{h}_1$ and $\mathbf{h}_2$ are the same, that is, $\{h_{1,k}\}_{k=1}^{K}$ and $\{h_{2,k}\}_{k=1}^{K} \in \{\beta_1, \beta_2, \ldots, \beta_K\}$. In practice, the estimates $\{\widehat{h_{1,k}}\}_{k=1}^{K}$ and $\{\widehat{h_{2,k}}\}_{k=1}^{K}$ are obtained independently in the case of; so, they are approximately equal. When $\mathbf{h}_1$ and $\mathbf{h}_2$ are obtained, we sort $\{\widehat{h_{1,k}}\}_{k=1}^{K}$ and $\{\widehat{h_{2,k}}\}_{k=1}^{K}$ in descending order, respectively, and have $\widehat{h_{1,1}} > \widehat{h_{1,2}} > \cdots > \widehat{h_{1,K}}$ and $\widehat{h_{2,1}} > \widehat{h_{2,2}} > \cdots > \widehat{h_{2,K}}$. Then, we can get the TOA estimates $\{\widehat{\tau_k}\}_{k=1}^{K}$ and $\{\widehat{\varsigma_k}\}_{k=1}^{K}$ according to the positions of nonzero values $\{\widehat{h_{1,k}}\}_{k=1}^{K}$ and $\{\widehat{h_{2,k}}\}_{k=1}^{K}$ in $\mathbf{h}_1$ and $\mathbf{h}_2$, and they are then paired.

4. Major Steps for Joint Estimation of TOA and DOA

Till now, we have achieved the proposal for joint TOA and DOA estimation in IR-UWB systems based on the sparse representation framework. We show the major steps of the proposed algorithm as follows:

1) Transform the transmitted and received signals into frequency domain and obtain $\mathbf{S}$, $\mathbf{Y}_1$, and $\mathbf{Y}_2$.
2) Construct overcomplete dictionary $\mathbf{E}$ and denote (6) and (7) by a sparse representation, which are shown in (13) and (14).
3) Recover the K-sparse vectors $\mathbf{h}_1$ and $\mathbf{h}_2$ via OMP algorithm and then the TOA estimates $\{\widehat{\tau_k}\}_{k=1}^{K}$ and $\{\widehat{\varsigma_k}\}_{k=1}^{K}$ can be determined from the sparse structure by plotting $\mathbf{h}_1$ and $\mathbf{h}_2$ on the grid of time samples.
4) Estimate the DOA estimates $\widehat{\theta_k}$ via (11).

***Remark 1*:** In practice, the information on the number of the multipath rays K is always unknown, but it can be estimated through some known techniques [35].

5. Advantages of Proposed Algorithm

The proposed algorithm has the following advantages:

1) The proposed algorithm can obtain paired TOA estimation, while the matrix pencil algorithm [18] cannot.
2) The proposed algorithm can work well with one single snapshot, which will be shown in section V.
3) The proposed algorithm has better parameter estimation performance than that of the matrix pencil algorithm, conventional PM algorithm, ESPRIT algorithm, and the algorithms in [19] and [20], which will also be shown in section V.

IV. CRB

In this section, we will derive the CRB of the joint-estimation performance based on the data model in the paper. According to [36] and [37], we can derive the CRB of TOA estimation as follows:

$$\mathbf{CRB}_{TOA} = \frac{\sigma_0^2}{2}\left[\mathrm{Re}\{\mathbf{D}^H \boldsymbol{\Pi}^{\perp}_{\mathbf{A}(\tau,\varsigma)} \mathbf{D} \odot \hat{\mathbf{P}}^T\}\right]^{-1}, \tag{21}$$

where σ_0^2 represents the noise power, $\mathbf{A}(\tau,\varsigma) = \begin{bmatrix}\mathbf{SE}_\tau \\ \mathbf{SE}_\varsigma\end{bmatrix}$, $\mathbf{D} = \left[\frac{\partial \mathbf{a}(\tau_1,\widehat{\varsigma_1})}{\partial \tau_1}\ \frac{\partial \mathbf{a}(\tau_2,\widehat{\varsigma_2})}{\partial \tau_2}\ \cdots\ \frac{\partial \mathbf{a}(\tau_K,\widehat{\varsigma_K})}{\partial \tau_K}\ \frac{\partial \mathbf{a}(\widehat{\tau_1},\varsigma_1)}{\partial \varsigma_1}\ \frac{\partial \mathbf{a}(\widehat{\tau_2},\varsigma_2)}{\partial \varsigma_2}\ \ldots\ \frac{\partial \mathbf{a}(\widehat{\tau_K},\varsigma_K)}{\partial \varsigma_K}\right]$, and $\mathbf{a}(\tau_k,\widehat{\varsigma_k})$ and $\mathbf{a}(\widehat{\tau_k},\varsigma_k)$ are the kth column of $\mathbf{A}(\tau,\hat{\varsigma})$ and $\mathbf{A}(\hat{\tau},\varsigma)$, respectively. The orthogonal projection matrix of A is $\boldsymbol{\Pi}^{\perp}_{\mathbf{A}(\tau,\varsigma)} = \mathbf{I}_{2M\times 2M} - \mathbf{A}(\tau,\varsigma)(\mathbf{A}(\tau,\varsigma)^H \mathbf{A}(\tau,\varsigma))^{-1}\mathbf{A}(\tau,\varsigma)^H$ and $\hat{\mathbf{P}} = \begin{bmatrix}\hat{\mathbf{P}}_s & \hat{\mathbf{P}}_s \\ \hat{\mathbf{P}}_s & \hat{\mathbf{P}}_s\end{bmatrix}$ with $\hat{\mathbf{P}}_s = \boldsymbol{\beta}\boldsymbol{\beta}^H$. Hadamard's product is represented by $\odot$.

From (21), we can rewrite the matrix $\mathbf{CRB}_{TOA}$ as $\mathbf{CRB}_{TOA} = \begin{bmatrix}\mathbf{CRB}_\tau & \kappa \\ \kappa & \mathbf{CRB}_\varsigma\end{bmatrix}$ with $\mathbf{CRB}_\tau$ being the CRB matrix of τ, and $\mathbf{CRB}_\varsigma$ being the CRB matrix of ς. The symbol κ denotes a part that is not considered in this paper.

According to (11), the CRB matrix of DOA can be expressed as

$$\mathbf{CRB}_{DOA} = \frac{\mathrm{c}^2}{d^2}\left(\mathbf{CRB}_\tau + \mathbf{CRB}_\varsigma\right)\left(\boldsymbol{\Psi}^{-1}\right)^2, \tag{22}$$

where $\boldsymbol{\Psi} = \mathrm{diag}([\cos(\theta_1), \ldots, \cos(\theta_K)])$ with θ_k, $k = 1, \ldots, K$ being the perfect DOA of the kth path.

V. Simulation Results

To assess the parameter estimation performance of the proposed algorithm, we present Monte Carlo simulations. Define the signal-to-noise ratio (SNR) and root-mean-square error (RMSE) as

$$SNR = 10\lg\frac{\|y(t)\|_F^2}{\|w(t)\|_F^2}, \tag{23}$$

Table 1. Simulation parameters.

Parameter	Value
Shape factor Γ	0.25 ns
Chip duration T_c	2 ns
Symbol duration T_s	10 ns
Modulation	BPSK
Frequency samples M	64
Number of multipath K	3
Channel-fading coefficients β_k	0.7, $0.4e^{-j\pi/2}$, 0.2
True estimates τ_k	0.3 ns, 0.46 ns, 0.62 ns
True estimates ς_k	0.2 ns, 0.3 ns, 0.5 ns
Space between the antennas d	10 cm
Distance between adjacent grids	0.002 ns

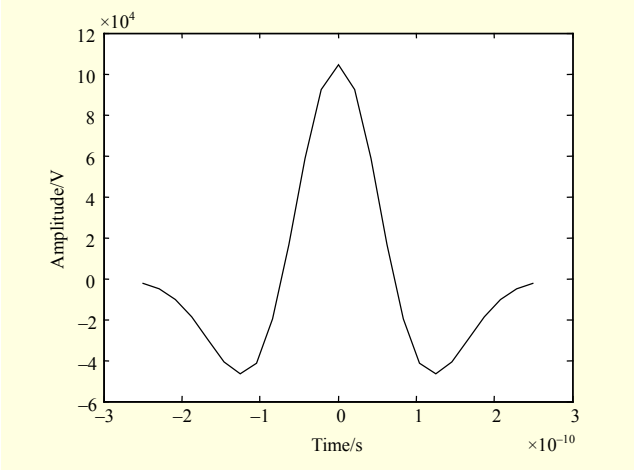

Fig. 3. UWB pulse waveform $p(t)$.

$$RMSE = \frac{1}{K}\sum_{k=1}^{K}\sqrt{\frac{1}{1000}\sum_{m=1}^{1000}\left|\widehat{\chi_{k,m}} - \chi_k\right|^2}, \quad (24)$$

where $y(t)$ is the received time-domain signal, $w(t)$ denotes the additive Gaussian white noise, and $\widehat{\chi_{k,m}}$ stands for the estimate of χ_k in the mth Monte Carlo trial. In the simulations, we assume the UWB pulse-wave function is $p(t) = \exp(-2\pi t^2/\Gamma^2)(1-4\pi t^2/\Gamma^2)$. The main simulation parameters are shown in Table 1. The shaping factor for the pulse is represented by Γ. The repetition of every symbol is $N_c = 5$, the chip duration is $T_c = 2$ ns, and the symbol duration is $T_s = N_c T_c = 10$ ns. We plot the transmitted BPSK-UWB signal $s(t)$ and the UWB pulse-wave function $p(t)$ in Figs. 3 and 4. Furthermore, we suppose that there are K=3 rays of BPSK-UWB arriving signals whose arrival times corresponding to the two antennas are $(\tau_1, \varsigma_1) = (0.3\text{ ns}, 0.2\text{ ns})$, $(\tau_2, \varsigma_2) = (0.46\text{ ns}, 0.3\text{ ns})$ and $(\tau_3, \varsigma_3) = (0.62\text{ ns}, 0.5\text{ ns})$, respectively. The UWB multipath channel-fading coefficients β_k are known with $\boldsymbol{\beta} = [0.7\ \ 0.4e^{-j\pi/2}\ \ 0.2]^T$, and there are M=64 frequency samples with the received signal. The grid distance between adjacent grids is 0.002 ns.

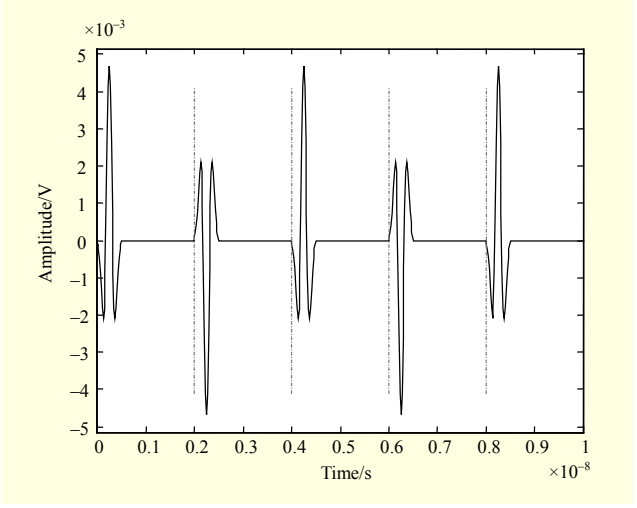

Fig. 4. Transmitted signal $s(t)$.

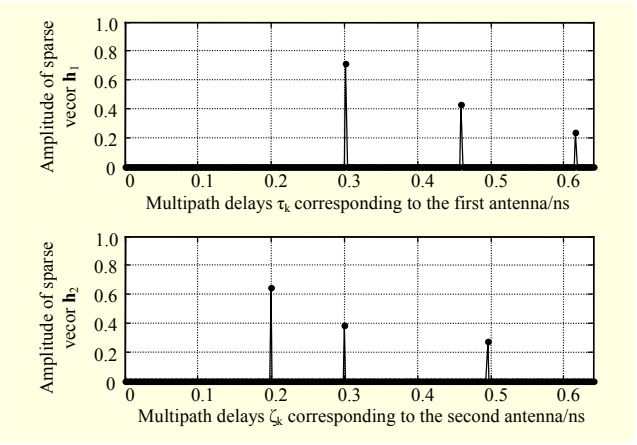

Fig. 5. TOA estimation with SNR=0 dB.

In Figs 5 and 6, we recover the sparse vectors $\mathbf{h}_1$ and $\mathbf{h}_2$ with different SNR and plot them on the grid of the time samples. Once $\mathbf{h}_1$ and $\mathbf{h}_2$ are obtained, the TOA estimates $\widehat{\tau_k}$ and $\widehat{\varsigma_k}$ are determined. Figures 5 and 6 illustrate that the elements of the sparse vectors and the estimation of TOA become more accurate in collaboration with SNR increasing.

Figures 7 and 8 show the TOA estimation results of the proposed algorithm over 50 Monte Carlo simulations with SNR = 0 dB and SNR = 10 dB. Figures 7 and 8 illustrate that our algorithm is effective for TOA estimation and the estimation precision improves as SNR increases.

Figures 9 and 10 present the TOA- and DOA-estimation performance of the proposed algorithm for different values of

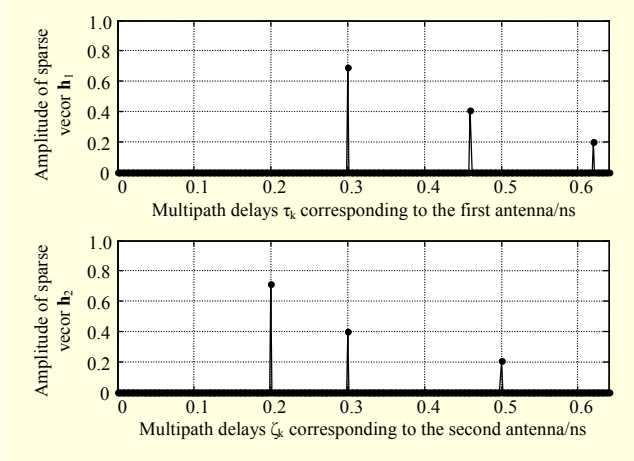

Fig. 6. TOA estimation with SNR=10 dB.

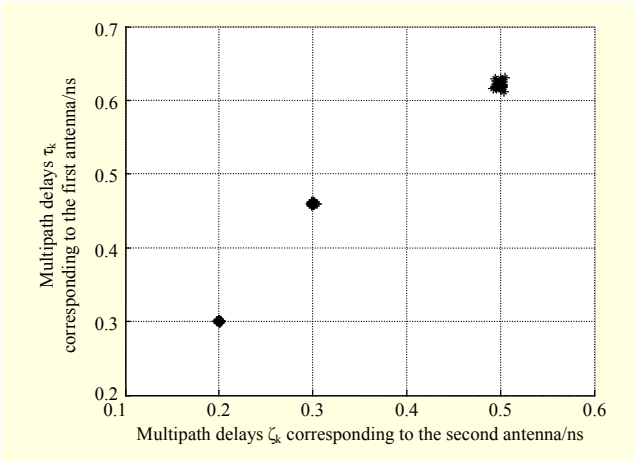

Fig. 7. TOA estimation with SNR=0 dB.

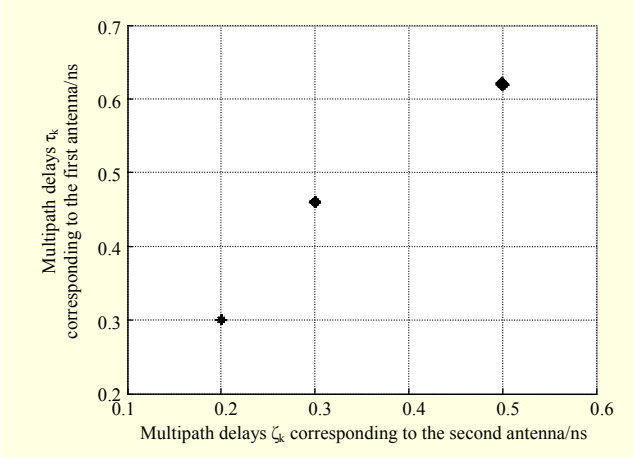

Fig. 8. TOA estimation with SNR=10 dB.

multipath K. It is indicated that the joint TOA and DOA estimation performance becomes better as K decreases.

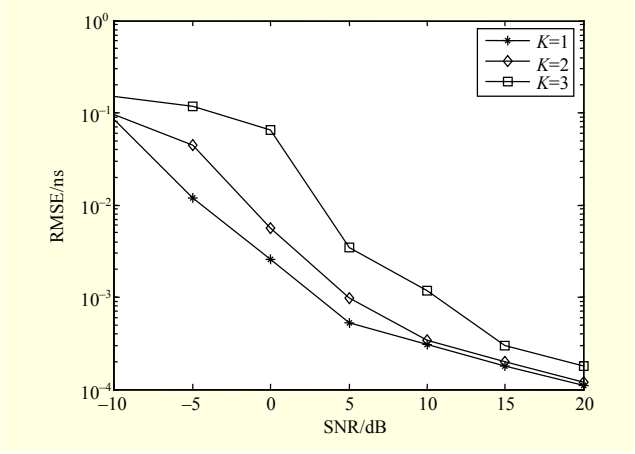

Fig. 9. TOA-estimation performance with different K.

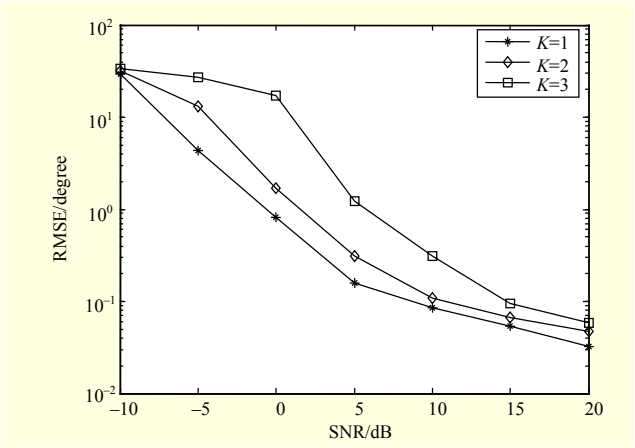

Fig. 10. DOA-estimation performance with different K.

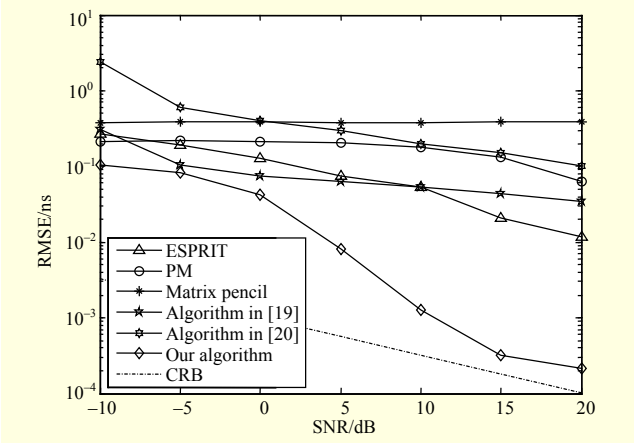

Fig. 11. TOA estimation comparison with different algorithms.

Figures 11 and 12 display the TOA- and DOA-estimation performance comparison of the proposed algorithm with the conventional PM algorithm [13], matrix pencil algorithm [18], ESPRIT algorithm, and other new joint estimation algorithms in [19] and [20] for the two antennas case. Note that the

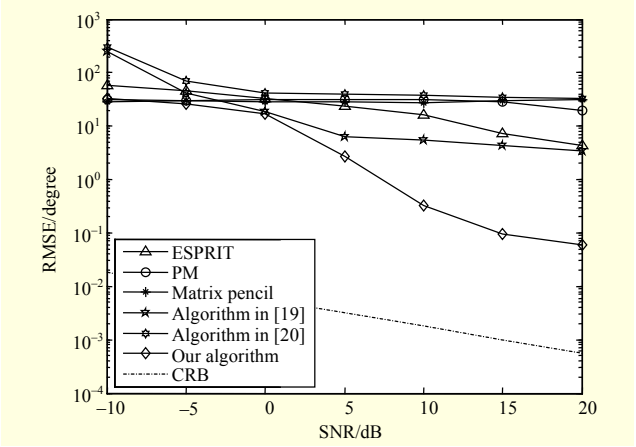

Fig. 12. DOA-estimation comparison with different algorithms.

ESPRIT algorithm is based on the data model in this paper and that all the algorithms are working under the condition of one single snapshot. From Figs. 11 and 12, we can draw the conclusion that the proposed algorithm has better joint TOA and DOA estimation performance than the conventional PM algorithm, matrix pencil algorithm, ESPRIT algorithm, and the algorithms in [19] and [20].

The conventional parameter-estimation algorithms PM, matrix pencil, and ESPRIT can all achieve reasonable estimation performances when collecting multiple snapshots. In the single snapshot condition, however, all these algorithms have poor estimation performances or even lose their effectiveness. Our algorithm is based on a sparse representation framework, where an l_0 norm optimization is used based on an OMP algorithm. It works well with one single snapshot and as such, our algorithm has better joint parameter-estimation performance than other algorithms.

VI. Conclusion

In this paper, we have presented a new formulation of the joint TOA and DOA estimation problem for IR-UWB signals in a sparse-signal representation framework, where a l_0 norm optimization is used based on an OMP algorithm. The proposed algorithm is able to estimate paired TOA and DOA parameters and has better joint TOA and DOA estimation performance than the conventional PM algorithm, matrix pencil algorithm, ESPRIT algorithm, and the algorithms in [19] and [20]. Numerical experiments illustrate the accuracy and efficacy of the proposed algorithm in a variety of parameters and scenarios.

References

[1] L. Yang and GB. Giannakis, "Ultra-wideband Communications: An Idea Whose Time Has Come," *IEEE Signal Process. Mag.*, vol. 21, no. 6, Nov. 2004, pp. 26–54.

[2] S. Gezici et al., "Localization via Ultra-wideband Radios: A Look at Positioning Aspects for Future Sensor Networks," *IEEE Signal Process. Mag.*, vol. 22, no. 4, July 2005, pp. 70–84.

[3] D. Dardari et al., "Ranging with Ultrawide Bandwidth Signals in Multipath Environments," *Proc. IEEE*, vol. 97, no. 2, Feb. 2009, pp. 404–426.

[4] H. Soganci, S. Gezici, and H.V. Poor, "Accurate Positioning in Ultra-wideband Systems," *IEEE Wireless Commun.*, vol. 18, no. 2, Apr. 2011, pp. 19–27.

[5] Y. Luo and C.L. Law, "Indoor Positioning Using UWB-IR Signals in the Presence of Dense Multipath with Path Overlapping," *IEEE Trans. Wireless Commun.*, vol. 11, no. 10, Oct. 2012, pp. 3734–3743.

[6] S. Wu et al., "Match-Filtering Based TOA Estimation for IR-UWB Ranging Systems," *Int. Conf. Wireless Commun. Mobile Comput.*, Crete Island, Greece, Aug. 6–8, 2008, pp. 1099–1105.

[7] S. Wu, Q. Zhang, and N. Zhang, "TOA Estimation Based on Match-Filtering Detection for UWB Wireless Sensor Networks," *J. Softw.*, vol. 20, no. 11, Nov. 2009, pp. 3010–3022.

[8] D. Dardari, C.-C. Chong, and M.Z. Win, "Threshold-Based Time-of-Arrival Estimators in UWB Dense Multipath Channels," *IEEE Trans. Commun.*, vol. 56, no. 8, Aug. 2008, pp. 1366–1378.

[9] A.A. D'Amico, U. Mengali, and L. Taponecco, "Energy-Based TOA Estimation," *IEEE Trans. Wireless Commun.*, vol. 7, no. 3, Mar. 2008, pp. 838–847.

[10] X. Li and K. Pahlavan, "Super-Resolution TOA Estimation with Diversity for Indoor Geolocation," *IEEE Trans. Wireless Commun.*, vol. 3, no. 1, Jan. 2004, pp. 224–234.

[11] C.-D. Wann and S.-H. Hsu, "Estimation and Analysis of Signal Arrival Time for UWB Systems," *IEEE Conf. Veh. Technol.*, Los Angeles, CA, USA, Sept. 26–29, 2004, pp. 3560–3564.

[12] J. Li et al., "Super-Resolution TOA Algorithm in Multi-path Environments," *Chinese J. Radio Sci.*, vol. 21, no. 5, Oct. 2006, pp. 771–776.

[13] H. Jiang, F. Cao, and R. Ding, "Propagator Method-Based TOA Estimation for UWB Indoor Environment in the Presence of Correlated Fading Amplitudes," *IEEE Int. Conf. Circuits Syst. Commun.*, Shanghai, China, May 26–28, 2008, pp. 535–538.

[14] K. Gedalyahu and Y.C. Eldar, "Time-Delay Estimation from Low-Rate Samples: A Union of Subspaces Approach," *IEEE Trans. Signal Process.*, vol. 58, no. 6, June 2010, pp. 3017–3031.

[15] F. Cao and M. Li, "Frequency Domain DOA Estimation and Tracking of UWB Signals," *Int. Conf. Wireless Commun. Netw. Mobile Comput.*, Chengdu, China, Sept. 23–25, 2010, pp. 1–4.

[16] V.V. Mani and R. Bose, "Direction of Arrival Estimation of Multiple UWB Signals," *Wireless Pers. Commun.*, vol. 57, no. 2, Mar. 2011, pp. 277–289.

[17] X. Mo, H. Jiang, and R. Qin. "Beamspace-Based DOA

Estimation of UWB Signal Using FDFIB Algorithm," *Recent Advances Comput. Sci. Inf. Eng*., Berlin: Springer Berlin Heidelberg, vol. 127, 2012, pp. 191–197.

[18] R. Ding, Z. Qian, and X. Wang, "UWB Positioning System Based on Joint TOA and DOA Estimation," *J. Electron. Inf. Technol*., vol. 32, no. 2, Feb. 2010, pp. 313–317.

[19] M. Navarro and M. Najar, "Frequency Domain Joint TOA and DOA Estimation in IR-UWB," *IEEE Trans. Wireless Commun*., vol. 10, no. 10, Oct. 2011, pp. 1–11.

[20] L. Taponecco, A.A. D'Amico, and U. Mengali, "Joint TOA and AoA Estimation for UWB Localization Applications," *IEEE Trans. Wireless Commun*., vol. 10, no. 7, July 2011, pp. 2207–2217.

[21] N. Laghmardi et al., "A Space-Time Extended MUSIC Estimation Algorithm for Wide Band Signals," *Arabian J. Sci. Eng*., vol. 38, no. 3, Mar. 2013, pp. 661–667.

[22] E.J. Candes, J. Romberg, and T. Tao, "Robust Uncertainty Principles: Exact Signal Reconstruction from Highly Incomplete Frequency Information," *IEEE Trans. Inf. Theory*, vol. 52, no. 2, Feb. 2006, pp. 489–509.

[23] D. Donoho, "Compressed Sensing," *IEEE Trans. Inf. Theory*, vol. 52, no. 4, Apr. 2006, pp. 1289–1306.

[24] J.L. Paredes, G.R. Arce, and Z. Wang, "Compressed Sensing for Ultrawideband Impulse Radio," *IEEE Int. Conf. Acoust*., *Speech Signal Process*., vol. 3, Apr. 2007, pp. 553−556.

[25] Z. Wang et al., "Compressed Detection for Ultra-wideband Impulse Radio," *IEEE Workshop Signal Process. Advances Wireless Commun*., Helsinki, Finland, June 17–20, 2007, pp. 1−5.

[26] H. Yao et al., "A Compressed Sensing Approach for IR-UWB Communication," *Int. Conf. Multimedia, Signal Process*., Guilin, China, May 14–15, 2011, pp. 3–7.

[27] J.L. Paredes, G.R. Arce, and Z. Wang, "Ultra-wideband Compressed Sensing: Channel Estimation," *IEEE J. Sel. Topics Signal Process*., vol. 1, no. 3, Oct. 2007, pp. 383–395.

[28] P. Zhang et al., "A Compressed Sensing Based Ultra-wideband Communication System," *IEEE Int. Conf. Commun*., Dresden, Germany, June 14–18, 2009, pp. 1–5.

[29] T. Liu, X. Dong, and W.-S. Lu, "Compressed Sensing Maximum Likelihood Channel Estimation for Ultra-wideband Impulse Radio," *IEEE Int. Conf. Commun*., Dresden, Germany, June 14–18, 2009, pp. 1–5.

[30] X.Y. Zhang, Y. Liu, and K. Wang, "Ultra Wide-Band Channel Estimation and Signal Detection through Compressed Sensing," *J. Xi'an Jiaotong Univ*., vol. 44, no. 2, Feb. 2010, pp. 88–91.

[31] T.N. Le, J. Kim, and Y. Shin, "An Improved TOA Estimation in Compressed Sensing-Based UWB Systems," *IEEE Int. Conf. Commun. Syst*., Singapore, Nov. 17–19, 2010, pp. 249–253.

[32] S. Wu et al., "High-Resolution TOA Estimation for IR-UWB Ranging Based on Low-Rate Compressed Sampling," *Int. ICST Conf. Commun. Netw*., Harbin, China, Aug. 17–19, 2011, pp. 478–483.

[33] A.A.M. Saleh and R.A. Valenzuela, "A Statistical Model for Indoor Multipath Propagation," *IEEE J. Sel. Areas Commun*., vol. 5, no. 2, Feb. 1987, pp. 128–137.

[34] J.A. Tropp and A.C. Gilbert. "Signal Recovery from Random Measurements via Orthogonal Matching Pursuit," *IEEE Trans. Inf. Theory*, vol. 53, no. 12, Dec. 2007, pp. 4655−4666.

[35] J. Xin, N. Zheng, and A. Sano, "Simple and Efficient Nonparametric Method for Estimating the Number of Signals without Eigendecomposition," *IEEE Trans. Signal Process*., vol. 55, no. 4, Apr. 2007, pp. 1405−1420.

[36] P. Stoica and A. Nehorai, "MUSIC, Maximum Likelihood, and Cramér-Rao Bound," *IEEE Trans. Acoust*., *Speech Signal Process*., vol. 37, no. 5, May 1989, pp. 720–741.

[37] P. Stoica and A. Nehorai, "Performance Study of Conditional and Unconditional Direction-of-Arrival Estimation," *IEEE Trans. Acoust*., *Speech Signal Process*., vol. 38, no. 10, Oct. 1990, pp. 1783−1795.

Fangqiu Wang was born in Hunan Province, China, on June 25, 1988. He is now a postgraduate student in the College of Electronic and Information Engineering, Nanjing University of Aeronautics and Astronautics, Nanjing, China. His research is focused on array signal processing and UWB communication.

Xiaofei Zhang received MS degree in electrical engineering from Wuhan University, Wuhan, China, in 2001. He received his PhD degree in communication and information systems from Nanjing University of Aeronautics and Astronautics, Nanjing, China, in 2005. Now, he is a professor at the College of Electronic and Information Engineering, Nanjing University of Aeronautics and Astronautics, Nanjing, China. His research is focused on array signal processing and communication signal processing.